

Evaluate synthesized nanoparticles as a good inhibitor for *Lactobacillus acidophilus*

Sara Habeeb Jassim,

Ali Essam Ali,

Shams Munaf Fathi

Alkarkh University Of Science

Abstract:

Magnesium oxide nanoparticles (MgO NPs) exhibit promising antibacterial properties, making them a potential solution for combating bacterial infections linked to dental caries. This research concentrated on assessing the impacts of MgO NPs on *Lactobacillus acidophilus*, specifically assessing their antibacterial activity. The assessment the research included observing the impacts of MgO nanoparticles (NPs) on bacterial proliferation suppression. Proliferation inhibition was assessed by calculating the percentage decline in the cloudiness of the bacterial solution and the decrease in bacterial colony development subsequent to exposure to MgO NPs. The inquiry demonstrated a dosage-dependent, noteworthy ($p < 0.05$) impeding of growth and effects on *Lactobacillus acidophilus* when subjected to 10–100 $\mu\text{g/ml}$ of MgO nanoparticles (NPs) across a 24-hour period. Fourier-transform infrared spectrometry (FTIR) analysis revealed that MgO NPs bond with polypeptides and glycogen in the microbial cell surface. Furthermore, Scanning electron microscopy (SEM) results emphasized the binding of MgO NPs to the cell wall, leading to its degradation and subsequent cellular damage. These findings confirm the bactericidal properties of MgO nanoparticles against *Lactobacillus acidophilus*.

Keywords: magnesium oxide nanoparticles, dental caries, *Lactobacillus acidophilus*, growth inhibition

Introduction

Green nanoscience's unique features enabled chemists and scientists to flourish swiftly. A nano technology deals with a small size of 1-100 nanometers, hence the particles termed nanoparticles (NPs) [1]. Nano particles of MgO used with low volume fraction to enhance the mechanical properties of epoxy Nano composite [2]. Altering the experimental procedures for synthesis opens up a fascinating world of possibilities, leading to a variety of shapes and sizes of Nanoparticles (NPs) crafted from a medley of compounds have become a hot topic in scientific discourse. Recently, there's been a remarkable pivot among researchers; they're embracing biological methods for synthesizing NPs rather than relying on the age-old physical or chemical techniques that have dominated the field. This refreshed

approach isn't just a fad—it's a conscious effort to ditch harmful toxins that come with traditional methods. Plus, it saves money! Who wouldn't want that? [3,4]. Imagine researchers successfully harnessing the power of nature—using extracts from leaves and flowers to create nanomaterials. It's not only an inspiring idea, but also a promising step toward sustainable innovation, but it also underscores the sustainable benefits of these innovative methods. [6,7]. Green techniques have been extensively advanced for the fabrication of MgO nanoparticles employing energy-efficient, economical, and sustainable methods. [8,9]. The goal of this research is to fashion magnesium oxide nanoparticles (MgONPs) via an eco-friendly synthesis method, employing Mg acetate as the initial precursor and citrus peels as the final outcome. Citrus peels can be utilized to reduce metal oxides such as ZnO, TiO₂, and so forth. Plant extracts function as oxidizing and reducing agents. [10, 11]. CITRUS peel is naturally light yellow. These peels completely cover the selected fruit inner portions from the outside environment. Additionally, water is used in this method to eliminate typical toxic chemicals. [12, 13]. Furthermore, warmth plays a pivotal role in the synthesis of magnesium oxide nanoparticles (MgO NPs). If thermal levels aren't quite right, it can mess with the phytochemicals, leading to the stabilization and reduction of these tiny particles. Equally, the balance and concentration of starting materials and extracts notably influence the magnitude and shape of MgO NPs. Furthermore, concerning the inorganic MgO substance, it is important to mention that it possesses a substantial band gap. [14]. It finds its way into various applications, from remediating toxic waste and serving catalytic purposes to material adsorption [15, 16], as well as reflecting and anti-reflecting coatings, and even in ionic batteries, among others [17,18]. MgO is utilized in healthcare for addressing heartburn, aiding bone healing [19], and alleviating stomach discomfort. MgO nanoparticles are considered a potential nanomaterial for cancer therapy. Many research endeavors have inspected the attributes and applications of MgO composites. For instance, Yamamoto determined that integrating MgO nanoparticles with various substances (like Ag, Zn, chitosan, phene, etc.) improved the stability and germicidal effectiveness of the compound. CS-MgO Nano composite films have demonstrated greater success in restraining microbial proliferation. [20]. Lactobacilli were chosen from twenty vaginal isolates obtained from twenty-five swabs taken from the vaginas of healthy married women [21]. The facility carried out the determination of these samples. Lactobacillus has been often associated with tooth decay 16. Nevertheless, the primary environmental element for the sustained existence of Lactobacilli

in the mouth seems to be the presence of decay. It is historically valuable to note that this link was verified by Harrison and Opal (1944) [22]. Presently, *Lactobacilli* remain viewed as an element in assessing the susceptibility to form cavities. As an initial phase in settlement, microbes affix to oral surfaces. [23]. The number of *Lactobacilli* was detected as significantly lowered in the saliva of people retaining sound oral states. While specific species of *Lactobacilli* were not linked to particular regions within the mouth, there were some species that could be identified in certain locations. [24] the isolated *Lactobacilli* from dental carries samples [25]. The chief characteristic of the genera *Lactobacillus* is acid production from fermentable sugars. Rodríguez Vargas(1921), had separated three types of the lactic acid microbes from dental caries, and he concluded that these species of *Lactobacillus* were accountable for generating acids that cause tooth decay [26].

Materials and Methods in research:

Citrus Peel Extract Preparation :

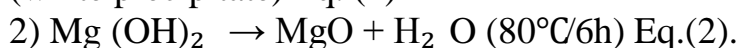
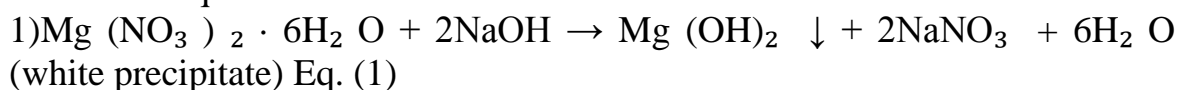
Citrus peel excerpts were made following the methodology detailed in the research [26]. Fresh citrus fruits were harvested from trees located in gardens throughout Baghdad. The peels were cleaned with distilled water to remove any dirt, then air-dried in the laboratory for 20 days to eliminate any remaining moisture before being ground into a fine powder for subsequent processing.

A total of 15 grams of the dried rind powder was heated under reflux in 250 milliliters of deionized water for (0.06) Molar one hour. The separation was carried out employing Whitman filter paper (0.1 μ m). The resulting filtered fluid was stored in the refrigerator for subsequent testing endeavors [1,3].

Magnesium Oxide Nanoparticles Synthesis:

For producing MgO NPs, one gram of Magnesium nitrate hexahydrate, was mixed in 50ml of deionized water inside a glass beaker. Afterward, 5ml of the priory prepared aqueous extract of peels was gradually introduced, employing a magnetic stirrer, for 6 hours to attain a consistent blend. The subsequent stage involved transforming the magnesium nitrate solution into MgO. A shift in color suggests the reduction process has taken place. One Normal sodium hydroxide solution (NaOH) was added slowly to maintain the solution pH at 12. Subsequently, the compound was warmed to 80 degrees Celsius for thirty minutes, at which juncture the nanoparticles formed and amassed at the base of the vessel. The mixture was then spun at 4,000 rotations per minute for four minutes, as shown in figure one. Ultimately, the MgO nanoparticles underwent a filtering process and were subjected to air

drying overnight, resulting in the formation of a white precipitate[37], as detailed in equations one and two below:



2.2. Exposure of bacteria to magnesium oxide nanoparticles (MgO NPs)

A decaying tooth was used to isolate *Lactobacillus acidophilus*, and the stock culture was kept at 37°C on De Man–Rogosa–Sharpe agar (MRS agar slant). To reach the stationary phase, the initial culture of *Lactobacillus acidophilus* was prepared from stock in sterile (De Man–Rogosa–Sharpe)MRS broth and incubated for 24 hours at 37°C. Fifty mL of fresh tryptic soy broth(TSB)was mixed with about 1 mL of primary culture, and the solution was allowed to stand for 4 hours at a heat of 37°C until it attained the mid-log growth phase. The initial solution was supplied as (150 µg/mL) and was then diluted with(De Man–Rogosa–Sharpe) MRS to yield four distinct concentrations of MgO NPs (10, 50, 75, and 100 µg/mL). Three-point five mL of MgO nanoparticles underwent mixing with 3.5 mL of bacterial culture at mid-log phase, possessing a starting absorbance of 0.03 at wavelength 600nm [38], for a duration of 24 hours at 37°C. The bacterial suspension exposed to the antibiotic Ampicillin (2.5 ml) served as the positive control, while the bacterial liquid without MgO NPs functioned as the negative control[39]..

Characterization of MgoNps

The bacterial suspension treated with the antibiotic Ampicillin (2.5 µg/ml) served as the positive control, while the bacterial solution without MgO NPs functioned as the negative control. To examine the crystalline features of the nanoparticles, X-ray diffraction (XRD) testing was carried out employing a Shimadzu XRD-600 instrument, operating at a voltage of 40 kV and employing CuK α radiation with a wavelength of 1.5405 Å across a broad spectrum of Bragg angles (30° ≤ 2θ ≤ 80°) across a wide range of Bragg angles. Fourier transform infrared (FT-IR) spectral evaluations were accomplished utilizing a Shimadzu IR-Prestige-21 spectrophotometer[40]. The effect of magnesium oxide nanoparticles on bacteria was evaluated through the turbidity method. A spectrophotometer (Shimadzu, IR-Prestige-21) measured the turbidity of bacterial cultures exposed to MgO NPs at a wavelength of 600 nanometers. Both positive and negative controls were kept at 37°C for 24 hours. To eliminate the interference caused by nanoparticles, The light attenuation at 600 nm of the MgO NPs suspension at various concentrations was gauged and taken away from the trial findings. The degree of bacterial

growth suppression from nanoparticle exposure was determined relative to the control cells, following Eq1.

$$I\% = \frac{\mu_C - \mu_T}{\mu_C} \times 100$$

Here are the definitions for each variable in the equation:

- **I%**: The percentage of bacterial growth inhibition.
- **μ_C** : The mean OD_{600} value of the control group (cells without nanoparticle exposure).
- **μ_T** : The mean OD_{600} value of the treatment group (cells with nanoparticle exposure).

Additionally, the bactericidal impact of MgO NPs was assessed using the colony count method. Using the streak plate method, bacterial cultures treated with MgO NPs for 24 hours (about 5 μ L) were plated on MRS along with a positive and negative control. After incubation for a day at 37°C, the plates were inspected to confirm whether the growth of microbial populations ceased by counting the colonies. Eq.1 was used to calculate the proportion of viable bacterial cells reduced compared to the control

2.6. Scanning electron microscopy (SEM) and energy-dispersive x-ray (EDX)

The attachment of MgO nanoparticles to the membrane of bacterial cells and the subsequent alterations in their shape were observed using scanning electron microscopy. Conversely, energy-dispersive X-ray spectroscopy was utilized to verify the elements or chemical makeup detected on the surfaces of the bacterial cells. The creation of nanoparticles was verified by the clear sharp peaks seen in the X-ray diffraction pattern of the magnesium oxide specimen; a lessening in the size of the nanoparticles was suggested by a widening of these peaks. Furthermore, the superior grade of the produced nanoparticles was confirmed by the absence of extra peaks. Centrifugation at 5000 rpm for 10 min was utilized to gather cells from a 10 mL solution of MgO NPs-treated cells. Following a series of alcohol washes (45, 95, and 100% ethanol), distilled water, 2.5% glutar aldehyde, and 0.01 M PBS, the pelleted bacterial cells were freeze-dried. SEM-EDX examination was performed on the freeze-dried bacterial cells.

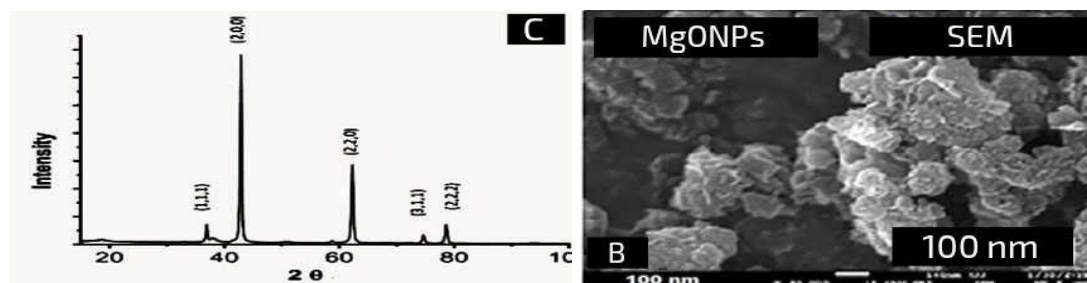


Figure 2- B. Analysis of MgO nanoparticles using scanning electron microscopy at a magnification of 50,000 times and X-ray diffraction (C).

2.7. Surface interplay of MgO NPs on microbes:

MgO NPs binding to the exterior of the bacteria was confirmed through Fourier transform infrared (FTIR) analysis, which identified the functional groups within the bacterial cell envelope responsible for this association. Bacterial cells were separated from 10 mL of bacterial broth treated with MgO NPs by spinning down at 6,000 rpm for a period of 10 minutes. To remove the moisture, the pelleted bacterial cells were freeze-dried after three rounds of washing with 1X PBS [27]. Fourier-transform infrared (FTIR) analysis was then carried out on the freeze-dried bacteria, covering the 4000–400 cm⁻¹ range.

3. Results & Discussion :

3.1 Characterization of MgO nanoparticles (NPs)

Dimensions and configuration of MgO NPs were assessed via SEM, and EDX scrutiny verified their elemental composition, as depicted in Fig. (2-A). The SEM evaluation suggested that the MgO NPs exhibited a mixture of hexagonal and stick-shaped particles, with dimensions ranging from 30.6 to 60.3 nm, and a mean size of 51.9 nm. The MgO NPs powder under review comprised magnesium and oxygen molecules, according to the EDX examination. The hexagonal structure of MgO NPs was confirmed by the XRD pattern in Figure (2-C).

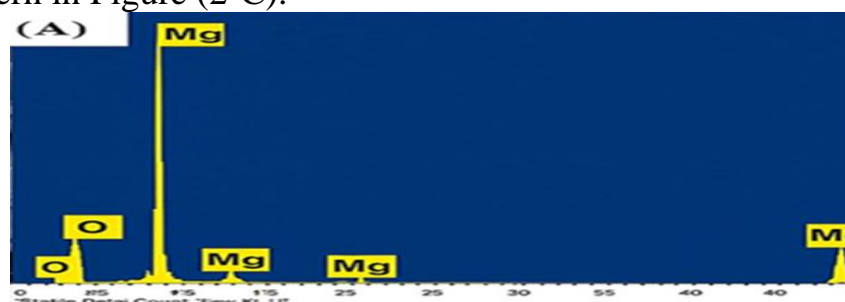


Figure (2-A). Characterization of MgO NPs under EDX.

3.2. A bacterial growth curve

Figure 3 depicts the *lactobacillus acidophilus* growth pattern. After 24 hours of incubation, the growth of lactobacillus decreased, and the log phase was detected between 3 and 6 hours of subculturing. The initial growth period of *lactobacillus acidophilus* commenced at 3 hours, succeeded by four hours of the middle proliferation stage, by eight hours the latter proliferation stage, and by nine hours the static phase in Todd-Hewitt broth supplemented with 0.2% yeast extract at 37 degrees Celsius. [28] displayed comparable progression patterns for *lactobacillus acidophilus* amid diverse growth conditions.

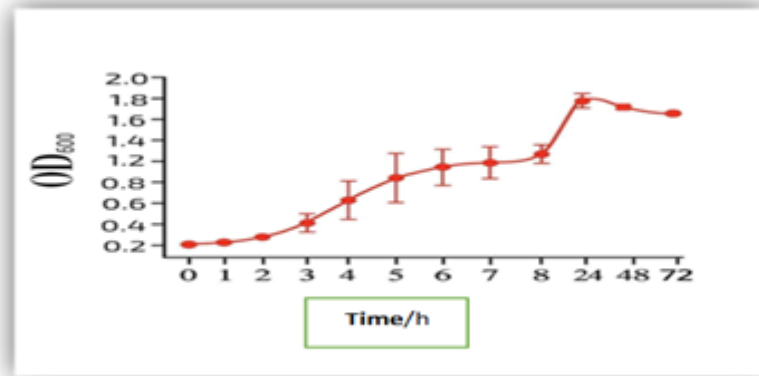


Figure 3:Growth curve of *lactobacillus acidophilus* in MRS broth at 37°C

3.3. Test for growth inhibition

The cloudiness of the bacterial culture was gauged to evaluate the growth-hindering actions of MgO NPs on lactobacillus tallying the bacterial colony subsequent to nanoparticles treatment. The lactobacillus culture's turbidity following 24 hours of incubation is depicted in Fig.4. With 10, 50, and 100 µg/mL of MgO NPs, the cloudiness of the bacterial suspension decreased by 40.50 ± 5.17 , 75.30 ± 7.01 , and $80.29 \pm 5.50\%$, correspondingly, based on the results. (Figure 4).

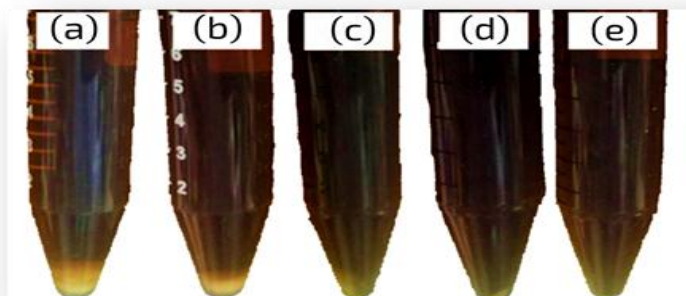
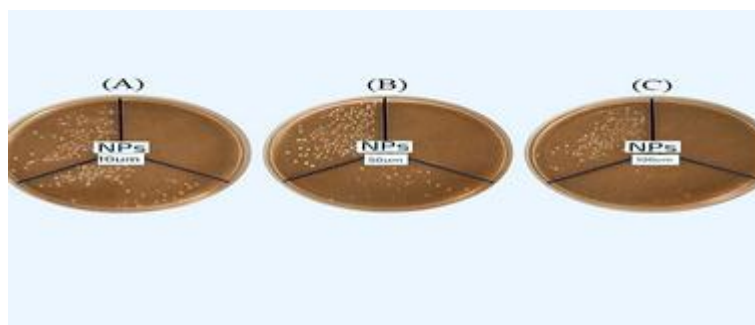


Figure 4 : The lessening of turbidity in lactobacillus within the broth (MRS) at 24 hours following exposure to 10 µg/mL (B), 50 µg/mL (C), and 100 µg/mL (D) of MgO nanoparticles is demonstrated. The negative and positive references are illustrated in (A) and (E) respectively.

At concentrations of 10, 50, and 100 µg/mL of MgO NPs, the colonies of MgO fell by 45 ± 5 , 94 ± 4 , and $97 \pm 5\%$, respectively, following 24 hours (Figure 4B). The lactobacillus cluster findings indicated a decrease in the amount of colonies as the MgO NPs' concentration rose. (Figure 5, Table



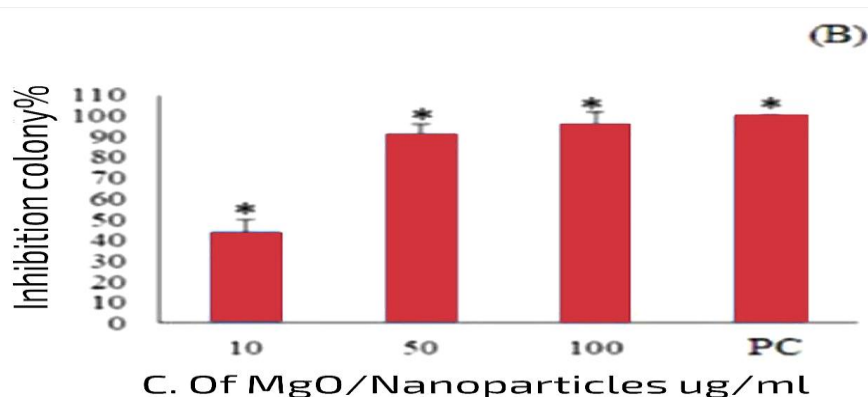
2). **Figure 5.** no. of colonies on (MRS) at 24h.

Table 2: no. of colonies on MRS at 24 h.

MgO NPs (µg/ml) calculator	bacterial colonies No. Mean ± Standard Deviation Calculator
0	180±4
10	100±7
50	16±5
100	5±3
Ampicillin (2.5µg)	0±0

Across all concentrations explored for MgO nanoparticles, the restraint of *lactobacillus acidophilus* development showed notable variations

(\$p < 0.05\$) when contrasted with the negative control, according to both colony enumeration and cloudiness evaluations. Consistent with our study, [29]. indicated an 85% decrease in the turbidity of the *Lactobacillus acidophilus* solution that was treated with 80 $\mu\text{g}/\text{mL}$ MgO nanoparticles after 10 hours, whereas [30] showed that *Lactobacillus* underwent over 95% growth suppression subsequent to exposure for 8 hours to concentrations spanning 310 to 550 $\mu\text{g}/\text{mL}$ of MgO



nanoparticles.

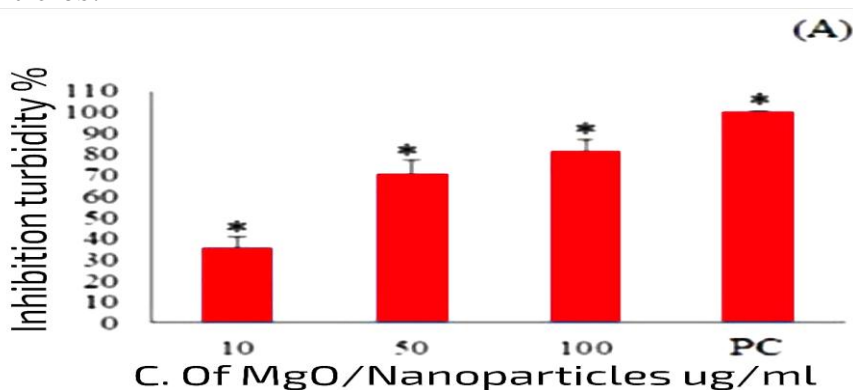


Figure 6: Share of growth inhibition tracked via turbidity of *Lactobacillus* cultures (A) and colony counting procedure (B) following exposure to differing amounts of MgO nanoparticles for 24 hours at 37 degrees Celsius in broth (MRS), along with positive control (PC). Shows a statistically significant variance between the control and the bacterial specimens subjected to MgO nanoparticles ($p < 0.05$).

3.5. Scanning electron microscopy (SEM) analysis:

Bacteria treated with MgO NPs showed a nearly five-fold higher magnesium content in their SEM EDX spectrum (Figure 7B) compared to the control (Figure 7D). Perhaps as a result of the magnesium in the culture media, the control sample had the lowest amount of magnesium. Phosphorus

might have been present in the bacterial growth substrate or rinse solution employed in the study, which is why there was a clear phosphorus peak in the test and control spectral readings (Figure 7B&D).

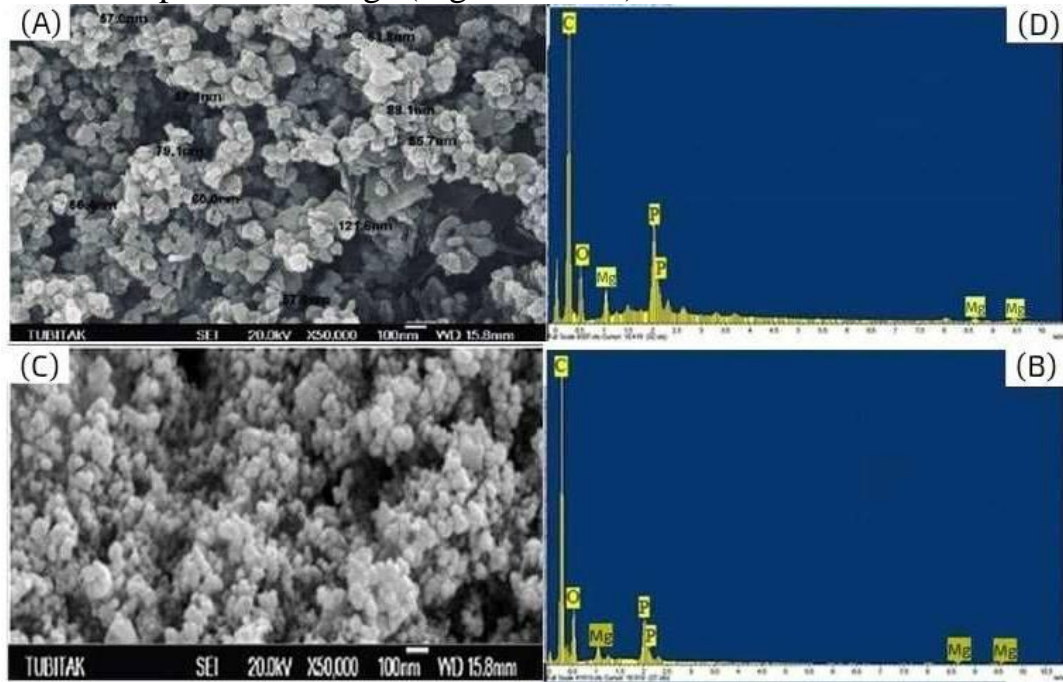


Figure 7: With magnification below 5,000X, SEM-EDX visuals display microbes subjected to a density of 100 μm of MgO nanoparticles for 24 hours, (C) and (D), beside the control baseline samples (A) and (B).

Results verified that MgO nanoparticles were gathering on the exterior of bacterial cells that were exposed to MgO nanoparticles. Furthermore, following a 24-hour exposure to 100 $\mu\text{g}/\text{ml}$ Regarding MgO nanoparticles, the bacterial suspension showed MgO NPs adherence onto the bacterial cell wall (Figure 8D), cell surface wrinkles (Figure 8C), and cell membrane rupture (Figure 8B).

An unbroken cell membrane and smooth, spherical cells were visible in the SEM picture of the control bacterial cells (Figure 8A) [31]. Comparable outcomes were observed in other research, like the breakdown of cellular membranes induced by MgO NPs handling and the subsequent outward flow of internal constituents in microbes. [32]. According to [31], "*lactobacillus acidophillus*" handled with 80 $\mu\text{g}/\text{ml}$ MgO nanoparticles (NPs) for 10 hours showed marked cell demise and alteration, with damaged cells situated near

the NPs,. After treating *E. coli* for 12 hours with 8 $\mu\text{g/ml}$ MgO NPs.

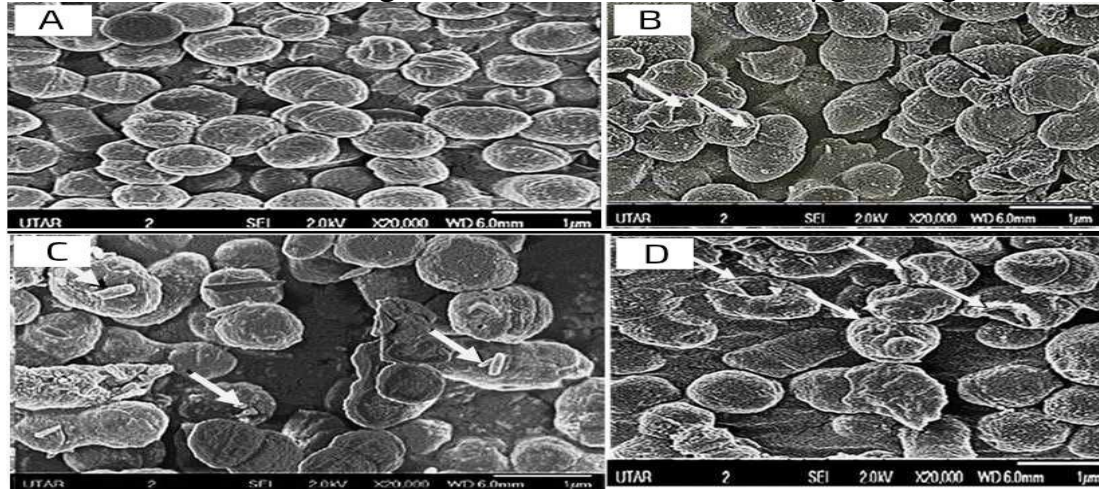


Figure 8 : SEM images of *Lactobacillus acidophilus* control (A) and bacterial cells treated with 100 μm MgO NPs at 24 hours reveal cell membrane rupture (B), bacterial cell surface distortion or wrinkles (C), and MgO NPs attachment to the cell membrane (D).

3.6. Surface interactions of magnesium oxide nanoparticles (MgO NPs) with bacterial cell walls

FTIR, was employed to investigate the functional groups that contributed to MgO NPs adherence on the surface of *lactobacillus acidophilus*, as depicted in Figure 9. A visual representation of MgO attachment is shown in Fig. 10. NPs to the cell walls of Gram-positive bacteria.

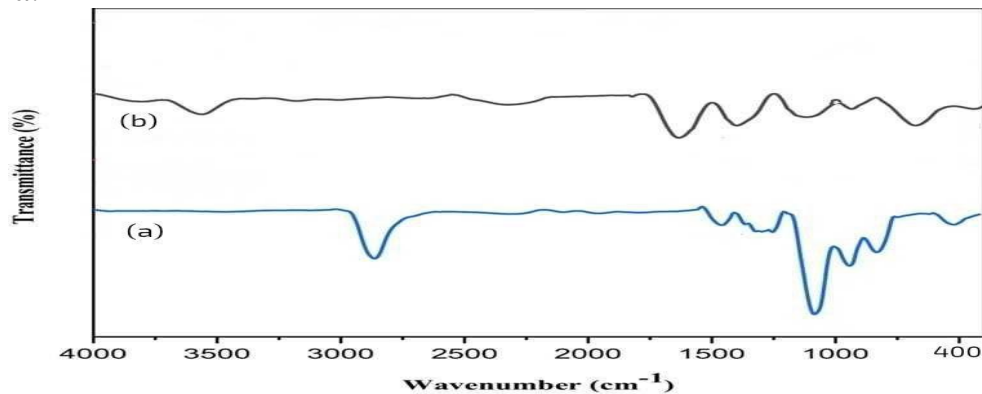


Figure 9 : FTIR of control (a) and 100 μm MgO NPs exposed *Lactobacillus acidophilus* (b).

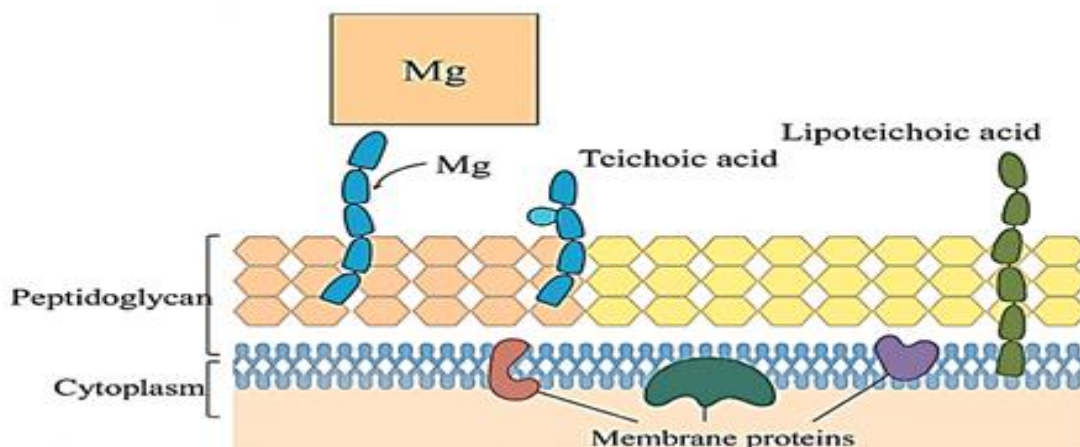


Figure 10: Visual representation of MgO NPs adhering to Gram-positive bacteria's cell wall.

The results were demonstrated by comparing the moved peaks between the control and MgO NPs at 100 $\mu\text{g/ml}$ that were exposed to bacterial cells for 24 hours. Magnesium oxide nanoparticles displaying intense peaks at 3415, 1633, 1500, and 434 cm^{-1} . The signals observed at the wavenumber of 3415 cm^{-1} suggested the presence of adsorbed O-H groups which aided in converting Mg acetate into Mg nanoparticles. Meanwhile, vibration of aromatic the C=O stretching of the polypeptide and protein framework was mainly ascribed to the area between are represented by the two bonds 1634 and 1550 cm^{-1} [33]. observed at 434 cm^{-1} confirmed the genesis of MgO Nano particles. Anionic groups on the bacterial cell wall and the cation Zn^{+} may have an electrostatic connection that causes MgO NPs to adhere to the cell wall. MgO NPs then bind to the bacterial wall and cell membrane, modifying the membrane potential and inducing the bacterial cell membrane to depolarize. MgO NPs then attach to the bacterial wall and cell membrane, modifying the membrane potential and inducing the bacterial cell membrane to depolarize. [34]. Membrane depolarization impedes respiration and energy transformation, generates an imbalance in the transport mechanism, and results in the loss of cell membrane soundness. Ultimately causes bacterial cells to rupture or expire [35]. Bacterial cell death might arise from the internal release of Mg^{2+} [35].

4. Conclusion

The results of the investigation demonstrated MgO NPs' influence on *lactobacillus acidophilus* via dose-dependent growth suppression. Moreover, it was verified that moieties from the bacterial cell wall polymers participated in the MgO NPs' surface adherence to the microbes. MgO NPs' linkage to the

bacterial cell lining. The findings demonstrated that magnesium nanoparticles have an effect on *Lactobacillus acidophilus* by disrupting its cell wall and killing it, thereby treating the dental cavities caused by this bacterium

References

- [1] Jassim, Sara H., and Taghried Ali Salman. "The potential of green-synthesized copper oxide nanoparticles from coffee aqueous extract to inhibit testosterone hormones." *Egyptian Journal of Chemistry* 65.4 (2022): 395-402.
- [2] Widad. Hamdi.J., and Safaa. Abed. S. "Comparing the Behaviors of ZrO₂ and MgO Nanoparticles in Mechanical Properties Improvement of epoxy composite." **The Journal of the College of Basic Education (CBEJ)** Vol. 24 No. 100 (2018) .
- [3] Salman, Taghried A., and Sara H. Jassim. "Zinc oxide nanomaterials as good inhibitors of steel corrosion in chloride solution." *AIP Conference Proceedings*. Vol. 2845. No. 1. AIP Publishing, 2023.
- [3] Jassim, Sara H., and Taghreed A. Salman. "The influence of green synthesized zinc oxide nanoparticles on testosterone hormone." *Clinical Risk* 5 (2006): 427.
- [4] Patil A. B., Bhanage B. M. Novel and Green Approach For The Nano crystalline Magnesium Oxide synthesis and its Catalytic Performance in Claisen– Schmidt Condensation. *Catal. Comm.*,36(5): 79-83 (2013).
- [6] Huang J., Li Q., Sun D., Lu Y., Su Y., Yang X., Wang H., Wang Y., Shao W., He N., Hong H., Chen C. Biosynthesis of silver and gold nanoparticles by novel sundried *Cinnamomum camphora* leaf C. *Nanotechnology* 18: 105-104 (2007).
- [7] Chandran S. P., Chaudhary M., Pasricha R., Ahmad A., Sastry M. Nanotriangles and silver nanoparticles using *Aloe vera* plant extract. *Biotechnol. Prog.*, 22: 577-583 (2006).
- [8] Deepak V., Kalishwaralal K., Pandian S. R. K., Gurunathan S. An insight into the bacterial biogenesis of silver nanoparticles, industrial production and scale-up in Rai M., Duran N. (Eds.): 'Metal nanoparticles in microbiology' (Springer-Verlag, Berlin, Chap. 2, 17–35 (2011).
- [9] Torrado A. M., Cortés S., Salgado J. M., Max B., Rodríguez N., Bibbins B. P., Converti A., Domínguez J. M. Citric Acid Production From Orange Peel Wastes By Solid-State Fermentation. *Brazil. J. Microbiol.*, 42: 394-409 (2011).
- [10] Sadeghi B., Rostami A., Momeni S. S. Facile Green Synthesis of Silver Nanoparticles Using Seed Aqueous Extract of *Pistacia atlantica* and its

Antibacterial Activity. *Spectrochimica Acta Part A: Molecular and Biomolecular Spectroscopy*, 134: 326-332 (2015).

[11] Logeswari P., Silambarasan S., Abraham J. Synthesis of silver nanoparticles using plants extract and analysis of their antimicrobial property. *J. Saudi Chem. Soc.*, 19: 311-317 (2015).

[12] Gaashani R., Radiman S., Al-Douri Y., Tabet N., Daud A. R. Investigation of the optical properties of Mg(OH)₂ and MgO nanostructures nanocryosurgical modality for tumor treatment using biodegradable MgO nanoparticles. *Nanomedicine* 8: 1233-1241 (2012).

[13] Ouraipryvan P., Sreethawong T., Chavadej S. Synthesis crystalline MgO nanoparticle with mesoporous-assembled structure via a surfactant modified sol-gel process. *Materials Lett.*, 63: 1862-1865 (2009).

[14] Bertinetti L., Drouet C., Combes C., Rey C., Tampieri A., Coluccia S., Martra, G. Surface characteristics of nanocrystalline apatites: Effect of MgO surface enrichment on morphology, surface hydration species, and cationic environments. *Langmuir*, 25: 5647-5654 (2009).

[15] Boubeta C. M., Bacells L., Cristofol R., Sanfeliu C., Rodriguez E., Weissleder R., Piedrafita S., Simeonidis K., Angelakeris M., Sandiumenge F., Calleja A., Casas L., Monty C., Martinez B. Self-assembled multifunctional Fe/MgO nanospheres for magnetic resonance imaging and hyperthermia. *Nanomedicine*, 6: 362-370 (2010).

[16] Di D. R., He Z. Z., Sun Z. Q., Liu J. A new nanocryosurgical modality for tumor treatment using biodegradable MgO nanoparticles. *Nanomedicine*, 8: 1233-1241 (2012).

[17] Fouda, A.; Hassan, S.E.-D.; Saied, E.; Azab, M.S. An eco-friendly approach to textile and tannery wastewater treatment using maghemite nanoparticles (γ -Fe₂O₃-NPs) fabricated by *Penicillium expansum* strain (K-w). *J. Environ. Chem. Eng.* **2020**, 9, 104693.

(18) Nguyen, N.T.T.; Nguyen, L.M.; Nguyen, T.T.T.; Tran, U.P.; Nguyen, D.T.C.; Van Tran, T. A critical review on the bio-mediated green synthesis and multiple applications of magnesium oxide nanoparticles. *Chemosphere* **2023**, 312, 137301.

[18] Jeevanandam, J.; Chan, Y.S.; Danquah, M.K. Cytotoxicity and insulin resistance reversal ability of biofunctional phytosynthesized MgO nanoparticles. *3 Biotech* **2020**, 10, 1-15.

- [19] Li, J.; Zhuang, S. Antibacterial activity of chitosan and its derivatives and their interaction mechanism with bacteria: Current state and perspectives. *Eur. Polym. J.* 2020, 138.
- [20] Lewkowicz X: *Erch Med Expt et anat path (Paris)* 1901; 13: 633-60.
- [21] Kawther Hkeem Ibrahim, and Sosan Hasan." Studying the ability of lactobacillus bacteria to inhibit the growth of uropathogens and their adhesion to uroepithelial cells" the *Journal of the College of Basic Education*. Dec 13, 2022.
- [22]. Harrison R and Opal Z: Comparative studies on Lactobacilli isolated from the mouth and intestine. *J Dent Res* 1944; 23: 1-22.
- [23]. Ahumada Mdel C, Bru E, Colloca ME, López ME, Nader-Macías ME. Evaluation and comparison of Lactobacilli characteristics in the mouths of patients with or without cavities. *J Oral Sci.* 2003 Mar;45(1):1-9. doi: 10.2334/josnusd.45.1. PMID: 12816358.
- [24] Cross ML, Stevenson LM, Gill HS. 2001. Anti-allergy properties of fermented foods: an important immunoregulatory mechanism of lactic acid bacteria? *Int Immunopharmacol* 1: 891-901. -
- [25] Caufield PW, Schon CN, Saraithong P, Li Y and Argimon S: Oral Lactobacilli and Dental Caries: A Model for Niche Adaptation in Humans. *J Dent Res* 2015; 94: 110S-118S.
- [26]. Rodríguez-Vargas FE: The specific study of the bacteriology of dental cavities. *Milit Dent J* 1921; 4: 199.
- [27]. Kamyar, Negin. Black Phosphorus Polymer Matrix Composites for Regenerative Medicine. Diss. The University of Manchester (United Kingdom), 2021.
- [28]. Yanfeng Tuo , Hanli Yu , Lianzhong Ai , Zhengjun Wu , Benheng Guo . ' Aggregation and adhesion properties of 22 Lactobacillus strains' *Journal of Dairy Science* Volume 96, Issue 7, July 2013, Pages 4252-4257.
- [29]. Zezhou Wu , Ann T.W. Yu , Liyin Shen , Guiwen Liu, " Quantifying construction and demolition waste: An analytical review" *Waste Management*, Volume 34, Issue 9, September 2014, Pages 1683-1692
- [30]. Krishna R Raghupathi, Ranjit T Koodali, Adhar C Manna, " Size-dependent bacterial growth inhibition and mechanism of antibacterial activity of zinc oxide nanoparticles" *Langmuir* 2011, 27, 7, 4020-4028. 2011.
- [31]. Yu Hang Leung, Alan M C Ng, Xiaoying Xu, Zhiyong Shen, Lee A Gethings, Mabel Ting Wong, Charis M N Chan, Mu Yao Guo, Yip Hang Ng, Aleksandra B Djurišić, Patrick K H Lee, Wai Kin Chan, Li Hong Yu, David Lee Phillips, Angel P Y Ma, Frederick C C Leung. " Mechanisms of

antibacterial activity of MgO: non-ROS mediated toxicity of MgO nanoparticles towards Escherichia coli" 17 December 2013.

[32]. I. W. Sutapa, A. Wahab, author N. L. Nafie. " Synthesis and Structural Analysis of Magnesium Oxide Nanomaterial Using Ethanol as Polymerization Solvent" Indonesia Journal of Materials Science Indonesia Journal of Fundamental and Applied Chemistry 2019.

[33]. Tahseen A. Ibrahim; Taghried A. Salman; Salma A. Abbas" Effectiveness of Magnesium oxide Nanoparticles in the Management of Thyroid Hormone Level" Egyptian Journal of Chemistry. Volume 64, Issue 6, June 2021, Pages 2889-2894.

[34]. Bhattacharya, Proma, Aishee Dey, and Sudarsan Neogi. "An insight into the mechanism of antibacterial activity by magnesium oxide nanoparticles." *Journal of Materials Chemistry B* 9.26 (2021): 5329-5339.

[35]. Nguyen, Nhu-Y. Thi, et al. "Antimicrobial activities and mechanisms of magnesium oxide nanoparticles (nMgO) against pathogenic bacteria, yeasts, and biofilms." *Scientific reports* 8.1 (2018): 16260.

[36]. Abdel-Aziz, Marwa M., Tamer M. Emam, and Elsherbiny A. Elsherbiny. "Bioactivity of magnesium oxide nanoparticles synthesized from cell filtrate of endobacterium Burkholderia rinojensis against Fusarium oxysporum." *Materials Science and Engineering: C* 109 (2020): 110617.

[37]. Singh J. P., Kim S. H., Kang H. K., Won S. O., Lee I.-J., Chae K. H. Are organic templates responsible for the optical and magnetic response of MgO nanoparticles? *Materials Chemistry Frontiers*, 2: 1707–1715 (2018)

[38]. Lee C, Lee K, Ha T, Choi JH, Kim SK, Chang H, Lee SW, Jang HD. Fabrication of 3D structured composites of crumpled graphene, polyaniline and molybdenum disulfide nanosheets for high performance alkali metal ion storage. *Advanced Powder Technology*. 2021 Feb 1;32(2):464-71.

[39]. Murtaza M, Aqib AI, Khan SR, Muneer A, Ali MM, Waseem A, Zaheer T, Al-Keridis LA, Alshammari N, Saeed M. Sodium alginate-based MgO nanoparticles coupled antibiotics as safe and effective antimicrobial candidates against Staphylococcus aureus of Houbara Bustard Birds. *Biomedicines*. 2023 Jul 11;11(7):1959.

[40]. Radulescu DM, Neacsu IA, Vasile BS, Surdu VA, Oprea OC, Trusca RD, Chircov C, Popescu RC, Ilie CI, Ditu LM, Drumea V. Green-Synthesized MgO Nanoparticles: Structural Insights and Antimicrobial Applications. *International Journal of Molecular Sciences*. 2025 Sep 16;26(18):9021.

تقييم الجسيمات النانوية المخلقة كمثبط جيد لبكتيريا

Lactobacillus acidophilus

ساره حبيب جاسم، علي عصام علي، شمس مناف فتحي
جامعة الكرخ للعلوم

مستخلص البحث:

استُخدمت جسيمات أكسيد المغنيسيوم النانوية (MgO NPs) في علاج الالتهابات البكتيرية في حشوات الأسنان نظراً لخصائصها المضادة للبكتيريا. هدفت هذه الدراسة إلى استكشاف التأثيرات المضادة للبكتيريا لجسيمات أكسيد المغنيسيوم النانوية على بكتيريا *Lactobacillus acidophilus*. قُيِّمت هذه الخصائص المضادة للبكتيريا من خلال دراسة تأثيرها على تثبيط النمو لجسيمات أكسيد المغنيسيوم النانوية على بكتيريا *Lactobacillus acidophilus*. حُدِّد تثبيط نمو البكتيريا من خلال نسبة انخفاض عكارة المُعلق البكتيري والمستعمرة البكتيرية عند المعالجة بجسيمات أكسيد المغنيسيوم النانوية. أظهرت النتائج تأثيراً معنوياً ($p < 0.05$) لتثبيط النمو وتأثيره على بكتيريا *Lactobacillus acidophilus* عند جرعة تتراوح بين 10 و100 ميكروغرام/مل من جسيمات أكسيد المغنيسيوم النانوية بعد 24 ساعة. أكد تحليل مطياف الأشعة تحت الحمراء بتقنية تحويل فورييه (FTIR) ارتباط جسيمات أكسيد المغنيسيوم النانوية بالبوليبينيدات والجليكوجين من جدار الخلية البكتيرية. كما أظهرت نتائج المجهر الإلكتروني الماسح (SEM) ارتباط جسيمات أكسيد المغنيسيوم النانوية بجدار الخلية البكتيرية، وما ينتج عن ذلك من تمزق في جدار الخلية وتلف للخلية. وأكدت نتائج الدراسة التأثيرات القاتلة لجسيمات أكسيد المغنيسيوم النانوية على بكتيريا *Lactobacillus acidophilus*.

الكلمات المفتاحية: جسيمات أكسيد المغنيسيوم النانوية، تسوس الاسنان، بكتيريا *Lactobacillus acidophilus* ، تثبيط النمو